Preprints of the 19th World Congress
The International Federation of Automatic Control
Cape Town, South Africa. August 24-29, 2014

Explicit Model Predictive Control of Bidirectional DC/DC Converter for Ultracapacitors Energy Storage Unit Applied to Light Rail Vehicle ⋆

Jianfeng Liu *,** **Qing Yan** *,** **Xiaohui Qu** *,** **Fei Jiang** *,**
Weirong Liu *,** **Zhiwu Huang** *,**

* *School of Information Science and Engineering, Central South University, Changsha, HUNAN 410075 China (e-mail: hzw@mail.csu.edu.cn)*
** *Hunan Engineering Laboratory for Advanced Control and Intelligent Automation, Changsha, HUNAN 410075 China*

Abstract: Ultracapacitors are popular as an energy storage device for the light rail regenerative power system. However, the control of the DC/DC converter is a challenging problem to meet the fast charging/discharging of ultracapacitors. In this paper, a precise discrete-time converter model and an explicit model predictive control scheme is proposed to address this issue. A converter model is presented by using a v-resolution method, which can capture the hybrid nature of the ultracapacitors in the form of piecewise affine. Based on this model, an optimal control problem with the constraints of the duty cycle and the system parameters is formulated. Then the control law is calculated by using multi-parameter programming. The resulting explicit solution can be easily stored and utilized in a lookup table. The proposed scheme can reduce the amount of on-line calculation and achieve the real-time control of the system. Simulation and experiment validate the effectiveness of the proposed scheme.

Keywords: ultracapacitors, fast charging/discharging, explicit model predictive control, v-resolution model, optimal control.

1. INTRODUCTION

Ultracapacitors, for its characteristics of long cycling life, fast charging/discharging rate, high power and energy density (Lerman et al., 2012; Karangia et al., 2013), are taken notably in light rail system as high power energy storage devices. By absorbing the regenerative braking energy and reusing it, the ultracapacitors energy storage system not only improves the energy efficiency but also stabilizes the voltage fluctuation of grid (Rufer et al., 2004; Lajnef et al., 2007).

For the ultracapacitors must be quickly charging or discharging with high instantaneous current (Allegre et al., 2010), the fast current and voltage reaction in the charging/discharging process are essential (Jae Sik Lim, 2010). However, the difficulties in controlling comes from their hybrid nature. According their two different models of operation, an associated linear continuous-time model would be established. So it is a challenging to include hard constraints when designing the controller with rapid dynamic response, for instance, the allowable operating voltage, and the range of the duty-cycle. Motivated by these issues, there has been a rising research interest in the energy storage unit control with the model predictive control (MPC).

Model predictive control has exhibited well performance in handling the multiple system constraints, and directly formulating an approximate model of the plant (Mo, Loh and Blaabjerg, 2011; Vahidi et al., 2006). But due to the small sampling period of such hybrid system, its rapidity and real-time should be highlighted. In (Yanhui Xie et al., 2009), a method to improve on-line computational efficiency is introduced for MPC scheme. By integrating some traditional methods like primal barrier method and infeasible start Newton method, a fast predictive controller can compute the control action much more efficiently than general MPC optimizer in (Yang Wang and Stephen Boyd, 2010). The finite control set model predictive control has been applied for current control (Rodriguez et al., 2007; Alireza Davari et al., 2012), in which the optimization problem can be reduced to predict the finite system behavior. However, these methods can possibly stuck into the local optimal point, and the optimal switching function set is considered in just one control cycle.

In this paper, a hybrid explicit model predictive control (EMPC) methodology (Petter THndela et al., 2003) based on a piecewise affine (PWA) equations is proposed, it can well meet the fast dynamic requirements and address the local optimization issues. In this control methodology, the system's constraints and objectives are taken into account

⋆ This work was partially supported by the National Natural Science Foundation of China (Grant Nos. 61203063, 61073103, 61003233 and 61379111).

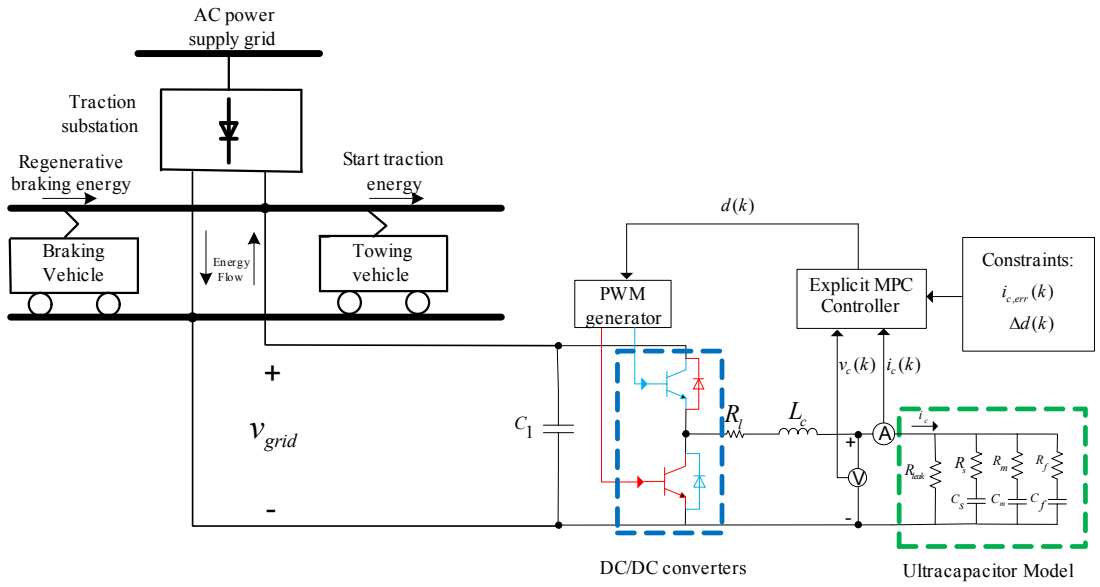

Fig. 1. The block diagram of bidirectional DC/DC converter for ultracapacitors energy storage system

based on the PWA mode. At the same time, consider the system which derived from the DC/DC converter's hybrid nature, we employ the v-resolution (Ferrari-Trecate et al., 2002) hybrid modeling techniques. It improves the accuracy of the system and captures the nonlinear behavior of the converter.

The key point of controller design is solving a constrained finite time optimal control (CFTOC) problem by using multi-parameter programming. In this paper, discharge current is taken as the cost function and the duty cycle range is taken as control constraints. From the proposed method, the optimal control problem would be pre-solved offline for every possible instance of the measured state, and which derived its explicit solution. The on-line computation is reduced to simply evaluating the optimal control law which has been saved in lookup table previous at each sampling instant.

This paper is organized as follows. In section 2, we briefly present the mathematical model and use the v-resolution modeling approach yields a discrete hybrid converter. Then formulate and solve a constrained finite time optimal control problem based on this model. Simulation and experimental results are shown in section 3, the EMPC scheme are tested in the energy storage unit that achieve the real-time optimization. Finally, conclusion and further research directions are outlined in section 4.

2. SYSTEM MODEL AND CONTROLLER DESIGN

Fig. 1 shows the ultracapacitors energy storage system of light rail vehicles. When the vehicle works in the braking phase, it leads to the grid voltage rise; the converter operates in buck mode charging the ultracapacitors. On the contrary, when the vehicle is in the acceleration or starting-up phase, the DC/DC converters change to the boost mode and energy is fed back to the grid through the boost inductor.

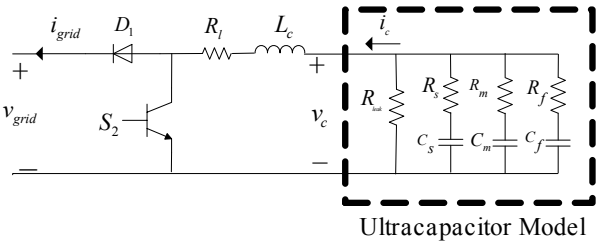

Fig. 2. The equivalent circuit of the DC-DC converter of ultracapacitors in the discharging state

In this paper, we have a detailed analysis when the ultracapacitors unit is in the discharging process, which means the topology operated as the boost mode; the buck operational mode of the system can be analyzed similarly.

2.1 Continuous-time Model of the Boost Mode

The equivalent model of the DC/DC converter connected with the ultracapacitors through a filtering inductance (L_c, R_l) is shown in Fig. 2, and R_l is the internal resistance of the inductor. The ultracapacitors is modeled by the RC equivalent circuit (Lisheng Shi and Crow, 2008), which $R_f, C_f, R_m, C_m, R_s, C_s$ are the resistances and capacitances of the fast, medium and slow branches respectively and R_{leak} is the leakage resistance.

The boost converter features two operation modes with two different affine dynamics, which can be described by

$$\begin{cases} L_c \dfrac{di_c}{dt} + R_l i_c = v_c, & kT_s \le t < (k + d(k))T_s \\ L_c \dfrac{di_c}{dt} + R_l i_c = v_c - v_{grid}, & (k + d(k))T_s \le t < (k+1)T_s \end{cases} \quad (1)$$

By taking $x_{cap} = [v_f \; v_m \; v_s \; i_c]^T$ as the state vector, where v_f, v_m, v_s is the capacitor voltage of each branch, i_c is the inductor current, v_c is the voltage of the ultracapacitors,

and v_{grid} is the grid voltage. The duty cycle $d(k) \in [0,1]$ in every switching period k, is chosen as the control input, and the switching period equal to T_s. Thus the system can be described by the following affine continuous-time state-space equations.

$$\begin{aligned} \dot{x}_{cap} &= \begin{cases} A_{cap}x_{cap}, & kT_s \le t < (k+d(k))T_s \\ A_{cap}x_{cap} + B_{cap}, & (k+d(k))T_s \le t < (k+1)T_s \end{cases} \\ y_{cap} &= C_{cap}x_{cap} \end{aligned} \quad (2)$$

where

$$x_{cap} = [i_c\ v_f\ v_m\ v_s]^T\ , y_{cap} = [i_c\ v_c\ ]^T,$$

$$A_{cap} = \begin{bmatrix} A_1 & A_2 \\ A_3 & A_4 \end{bmatrix},$$

$$A_1 = \begin{bmatrix} \frac{-R_z - R_l}{L_c} & \frac{R_z}{R_f L_c} \\ \frac{-R_z}{R_f C_f} & (\frac{R_z}{{R_f}^2 C_f} - \frac{1}{R_f C_f}) \end{bmatrix},$$

$$A_2 = \begin{bmatrix} \frac{R_z}{R_m L_c} & \frac{R_z}{R_s L_c} \\ \frac{R_z}{R_f C_f R_m} & \frac{R_z}{R_f C_f R_s} \end{bmatrix},$$

$$A_3 = \begin{bmatrix} \frac{-R_z}{R_m C_m} & \frac{R_z}{R_m C_m R_f} \\ \frac{-R_z}{R_s C_s} & \frac{R_z}{R_s C_s R_f} \end{bmatrix},$$

$$A_4 = \begin{bmatrix} (\frac{R_z}{{R_m}^2 C_m} - \frac{1}{R_m C_m}) & \frac{R_z}{R_m C_m R_s} \\ \frac{R_z}{R_s C_s R_m} & (\frac{R_z}{{R_s}^2 C_s} - \frac{1}{R_s C_s}) \end{bmatrix}.$$

$$R_z = \left(\frac{1}{R_f} + \frac{1}{R_m} + \frac{1}{R_s} + \frac{1}{R_{leak}}\right)^{-1}$$

$$B_{cap} = \begin{bmatrix} -\frac{v_{grid}}{L_c} & 0 & 0 & 0 \end{bmatrix}^T$$

$$C_{cap} = \begin{bmatrix} 1 & 0 & 0 & 0 \\ -R_z & \frac{R_z}{R_f} & \frac{R_z}{R_m} & \frac{R_z}{R_s} \end{bmatrix}$$

2.2 v-Resolution Discrete-Time Hybrid Model

In contrast to the average state space model, the formulation of the model is natural in the discrete-time domain, which improves the accuracy of the model and achieves much smaller error. The details can be seen in (Mayne and Rakovi, 2003).

The period of the pulse width modulation T_s is divided into v sub-periods of the $\tau_s = T_s/v, v \in N, v \ge 1$ as showed in Fig. 3. And within the kth period, we use $\xi_{cap}(n)$ to denote the states at time-instants $KT_s + n\tau_s, n \in \{0,1,...v-1\}$. By definition, $\xi_{cap}(0) = x_{cap}(k), \xi_{cap}(v) = x_{cap}(k+1)$. For each subperiod, we introduce mode one and mode two previously discussed and plus an additional mode three that captures the transition from mode one to mode two (Tobias Geyer et al., 2008). In the nth subperiod, the state-update equation is

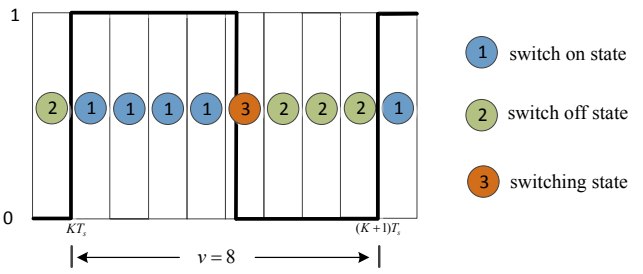

Fig. 3. v-resolution modeling approach visualized for the kth period (the example using $v = 8$ and each mode means the position of the switch)

$$\xi_{cap}(n+1) = \begin{cases} \Phi_{cap}\xi_{cap}(n), & d(k) \in [0, \frac{n}{v}) \\ \Phi_{cap}\xi_{cap}(n) + \Psi_{cap}(vd(k) - n), & \\ \qquad \frac{n}{v} \le d(k) \in [\frac{n}{v}, \frac{n+1}{v}) & \\ \Phi_{cap}\xi_{cap}(n) + \Psi_{cap},\ d(k) \in [\frac{n+1}{v}, 1] & \end{cases} \quad (3)$$

where Φ_{cap} and Ψ_{cap} are the discrete-time representations of A_{cap} and B_{cap} which defined in (1) with sampling time τ_s, and the mode three is a weighted average of the modes one and two.

For the control law depicted as the form of explicit function, in general, the model should be linear or piecewise affine (PWA), which can be written as

$$x(k+1) = A_i x(k) + B_i d(k) + f_i;\ \ i = 1, 2.....v \quad (4)$$

Where A_i, B_i and f_i are constant matrices. So that it can partition the state-input space into polyhedra and associate with each polyhedron an explicit output solution (Anders Rantzer and Mikael Johansson, 2000).

The discrete-time state-update map of the v-resolution model can be derived using (3) by the form of (4). From $x_{cap}(k) = \xi_{cap}(0)$ to $x_{cap}(k+1) = \xi_{cap}(v)$, the state-update function maps the sampled state $x_{cap}(k)$ from time in stant kT_s to time instant $(k+1)T_s$. In this paper, we set $v = 3$, the boost operational mode of the system can be depicted as

$$x_{cap}(k+1) = {\Phi_{cap}}^3 x_{cap}(k) + \begin{cases} 3{\Phi_{cap}}^2\Psi_{cap}d(k), & d(k) \in [0, \frac{1}{3}) \\ 3\Phi_{cap}\Psi_{cap}[d(k) - \frac{1}{3}] + {\Phi_{cap}}^2\Psi_{cap}, & d(k) \in [\frac{1}{3}, \frac{2}{3}) \\ 3\Psi_{cap}(d(k) - \frac{2}{3}) + {\Phi_{cap}}^2\Psi_{cap} + \Phi_{cap}\Psi_{cap}, & \\ \qquad d(k) \in [\frac{2}{3}, 1] & \end{cases} \quad (5)$$

2.3 Constrained Finite Time Optimal Control Scheme

The main control objective is to regulate the inductor current i_c of the light rail regenerative energy storage systems with ultracapacitor to its reference $i_{c,ref}$. In this paper, we want the inductor current charge as soon as possible. This regulation has to be achieved in the presence of the hard constraints on the manipulated variable (the duty cycle) which is bounded between 0 and 1, in addition, with the v_c be controlled between 500V and 1000V. Moreover, the controller must render a steady state operation under a

constant duty cycle, thus avoiding the occurrence of fast-scale instabilities.

In this paper, we assume the load capacitive reactance is time invariant and nominal. In order to regulate the discharge current to its reference current quickly and with overshoot as little as possible. It is to minimize the current error $i_{c,err}$, and to respect the constraints on the ultracapacitors voltage and the duty cycle.

$$i_{c,err}(k) = \sum_{n=0}^{v-1} \frac{i_c(n) + i_c(n+1)}{2v} - i_{c.ref} \tag{6}$$

Additionally, let $\Delta d(k) = |d(k) - d(k-1)|$ indicate the absolute value of the difference between two consecutive duty cycles. This term is introduced in order to reduce the presence of unexpected high input fluctuation when the system has almost reached stationary conditions.

Define the penalty matrix $Q = diag\{q_1, q_2\}$ and the vector $\varepsilon(k) = [i_{c,err}(k), \Delta d(k)]^T$. Then the objective function can be defined as:

$$\begin{aligned} J(x_{cap}(k), \Delta d(k)) &= \sum_{i=0}^{N-1} \|Q\varepsilon(k+i)|\, k)\|_2 \\ s.t \qquad & 0 \le d(k) \le 1 \\ & i_{c,\min} \le i_c(k) \le i_{c,\max} \\ & v_{c,\min} \le v_c(k) \le v_{c,\max} \end{aligned} \tag{7}$$

Where the N means the predictive horizon and the index will penalize the predictive evolution error using the 2-norm. This paper, we get the parameter vector.

$$p(k) = [v_f(k)\ v_m(k)\ v_s(k)\ i_c(k)\ d(k-1)] \tag{8}$$

The control input at time-instant k is then obtained by minimizing the objective function (6). Starting from the measured state vector $x_{cap}(k)$ from the state equation. The sequence of control moves $D(k) = [d(k), ..., d(k+L-1)]^T$ subject to the model and constraints. The associated optimization program is referred to as the constrained finite time optimal control (CFTOC) problem (Borrelli, 2003). The resulting optimal control input $d^*(k)$ at instant k is then applied to the converter and the procedure repeated at the successive sampling instant with new state $x_{cap}(k+1)$.

2.4 The State Feedback Control Law

Multi-parametric programming(Tondel et al., 2003) is used to solve an optimization problem offline for a range of parameters. In this paper, it solves a discrete-time CFTOC problem for a PWA system by this multi-parametric program (Baotic et al., 2003) with the parameters vector (7).

The CFTOC problem is not only a parametric function of the physical state, but also depends on the last control input $d(k-1)$, as the changes of the duty cycle are penalized in the objective function; it is necessary to solve the CFTOC problem for possible values of $i_{c,ref}$. The optimal state-feedback control law $d^*(k)$ is a PWA function of the state vector, it defined on a polyhedral partition of the feasible (augmented) state space, and can be expressed as

$$d^*(k) = F_j x_t(k) + G_j \tag{9}$$

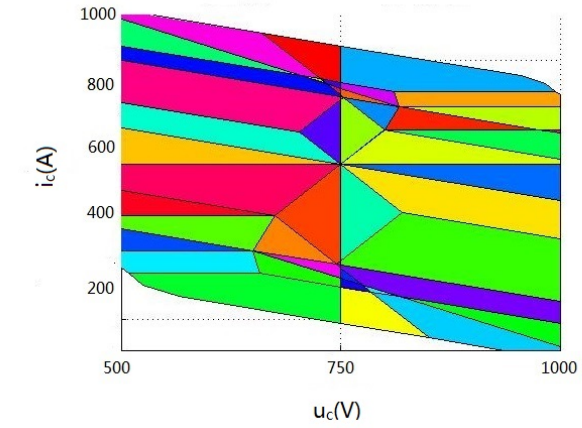

(a)

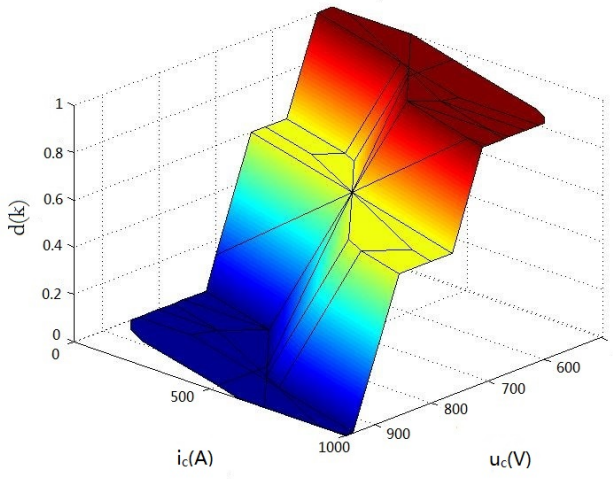

(b)

Fig. 4. The state partitions and state feedback control law for $d(k-1) = 0.6$, V_s= 995 V and V_m= 950 V, where dark blue corresponds to $d(k) = 0$ and dark red to $d(k) = 1$. (a) PWA control partitions u_c, i_c, where the $u_c = v_f$. (b) State feedback control law d(k).

$$H_j x(k) \le K_j \quad j = 1...P \tag{10}$$

Where H_j and K_j define the jth of the regions in the polyhedral partition of the controller andF_j, $G_j$associate with the piecewise affine control law.

The obtained state-feedback controller is implemented online. By computing the control input amounts and determine the polyhedron in which the measured state lies. At last, check (10) and simply evaluate the corresponding affine control law(9).

As the set of converter parameters show in Table 1 and the controller parameters show in Table 2. The final result of the optimal state-feedback control law is a PWA function defined on a polyhedral partition of the 5-D parameter space, of which the v_s and v_m vary in a small range. Therefore, using the complexity reduction algorithm (Geyer et al., 2004), the controller is simplified

to 33 regions, to visualize the state-feedback control law, fixed $d(k-1)$, $v_s = 995V$ $v_m = 950V$. We compute the state-feedback control using the multiparametric toolbox (Kvasnica et al., 2004). Now the 2-D space shown in Fig. 4(a) depicts the regions of lookup table and Fig. 4(b) show the control input $d(k)$ as a PWA function of $x(k)$.

Table 1. Converter parameter setting

parameter	value	parameter	value
R_l	0.1Ω	L_c	0.56MH
R_f	0.03Ω	R_{leak}	31.15kΩ
R_S	107.13Ω	R_m	40.92Ω
C_m	35.16F	C_s	8.26F
C_f	35F		

Table 2. Controller parameter setting

parameter	value	parameter	value
v	3	N	2
q_1	4	q_2	0.3
f_s	1kHZ		

3. SIMULATION AND EXPERIMENTAL RESULT

3.1 Simulation

In this section, the EMPC controller is evaluated in simulation for variations in the inductor current is presented. The simulation set up was built using Matlab/Simulink. Where the parameters has been given in Table 1. We have considered the scenario where the reference inductor current with the value of $i_{ref} = 1000A$.

We uses the same parameters as the physical plant model. The choice of $v = 3$ subperiods make the v-resolution model captures the nonlinear discrete-time dynamics in a sufficiently accurate way.

The simulation response of the system is illustrated in Fig. 5. And we assume all the parameters are measured. Where Fig. 5(a) show the inductor incurrent, Fig. 5(b) show the variations of the capacitor voltage. At the beginning, the voltage is stabilized and the inductor current raised for which the EMPC controller been used. As show in Fig. 5(c), the controller switches the duty cycle in order to perform a good tracking of the reference and also guarantee the systems constraints. While after only about 30 ms, the controller is stabilizing. So it is easy to see that the system's stabilizing time is rising fastly for the EMPC controller.

3.2 Experimental Results

The proposed controller in this paper has been implemented in a light rail vehicle's energy storage system, which verified the algorithms effectiveness. System parameters have been defined as follows: the ultracapacitors are 400 cells in series of each capacitor 3500F with ESR 9.8mΩ, and the convert switching frequency is $1k$HZ. Regarding the optimal scheme, the penalty matrix chosen to be $Q = diag\{4, 0.3\}$, getting a small weight on the changes of the manipulated variables.

The response of the current and voltage in both charging, discharging process are shown at Fig.6. As can be seen

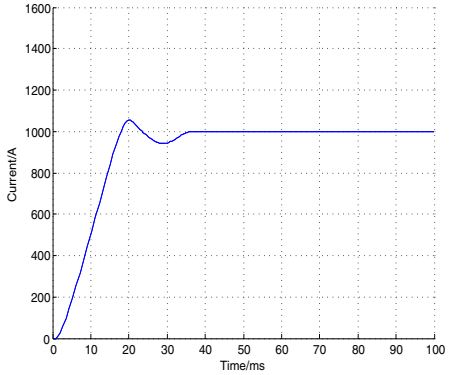

(a)

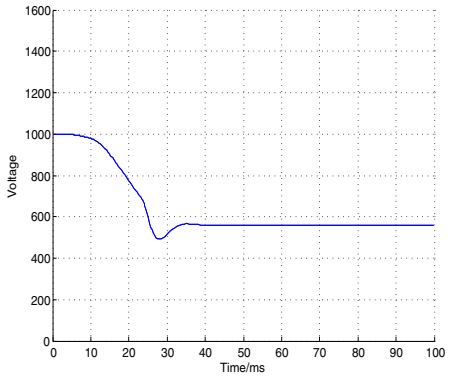

(b)

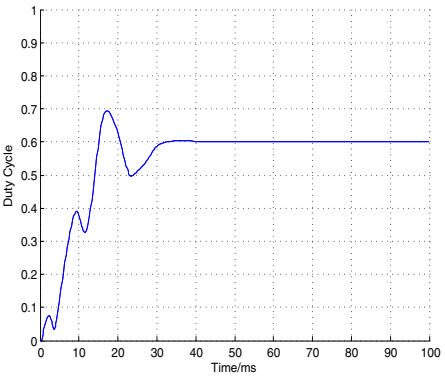

(c)

Fig. 5. Simulation results. (a) inductor current. (b) variations of the capacitor voltage. (c) the duty cycle.

from $0km/h$ to $60km/h$, the controller increase the inductor current and decrease the output voltage, the constrains is reached to discharge the ultracapacitors to the reference inductor current as fast as possible. Once the inductor current reaches its reference, the ultracapacitors quickly discharge its energy and the voltage to the limit value to avoid any overshoot.

The hybrid nature of the system is reflected by using the EMPC controller, as show from the experimental results, its fast response are not degraded compared with the results of the simulation. In the presented case, both the simulation and experiment of the converter is made at a small frequency of 1KHz, which slows down the closed-loop systems dynamics. The differences between the simulation and experimental results can be reduced when the DC/DC

converters operating at a higher frequency. So when the DC/DC converter operating at a higher fixed-frequency, the control scheme can satisfy its requirement of rapidity and real-time better.

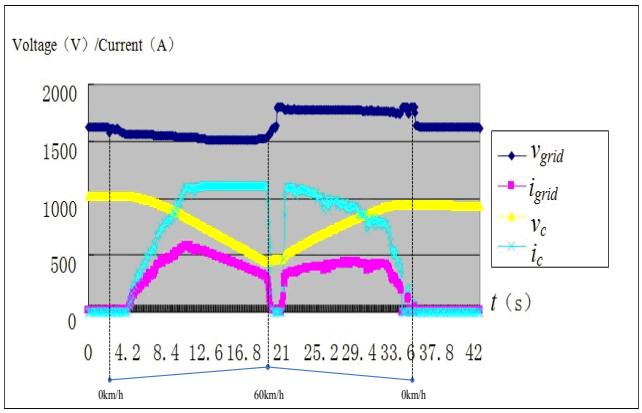

Fig. 6. Experimental results of the grid voltage v_{grid}, gird current i_{grid}, ultracapacitors voltage v_c and ultracapacitors charging/discharging current i_c with the vehicle speed from 0 km/h to 60 km/h, and 60 km/h to 0 km/h.

4. CONCLUSION

In this paper, an explicit model predictive control scheme is proposed for ultracapacitors energy storage system. Due to its hybrid nature of the DC/DC converter, an extension of the v-resolution model is developed to describe its topology in the form of piecewise affine. The controller can be based on this model, and is derived. The calculation of the explicit control law is a constrained finite time optimal control problem. It was solved by using multi-parametric programming offline. The proposed EMPC makes it feasible to incorporate the hard physical constraints on the duty cycle and reduced the online computational complexity. The state-feedback controller is of piecewise affine form, which can be used by an effective lookup table. The experimental results demonstrated that the controller could respond to fast current changes, and could make the grid voltage to adapt to the load changes rapidly. The design guideline and stability analysis of the proposed EMPC will be the future work.

REFERENCES

C. Lerman et al. Capacitor semi-active battery-ultracapacitor hybrid energy source. *In IEEE 2012 27th Convention of Electrical and Electronics Engineers in Israel*, 1-4, 2012.

R. Karangia et al. Battery-supercapacitor hybrid energy storage system used in Electric Vehicle. *In International Conference on Energy Efficient Technologies for Sustainability (ICEETS)*, 688-691, 2013.

A. Rufer et al. A Supercapacitor-Based Energy Storage Substation for Voltage Compensation in Weak Transportation Networks. *IEEE Transactions on Power Delivery*, 19(2), 629-636, 2004.

W. Lajnef et al. Characterization methods and modeling of ultracapacitors for use as peak power sources. *Journal of Power Sources*, 168(2), 553C560, 2007.

Allegre A L et al. Energy Storage System With Supercapacitor for an Innovative Subway. *IEEE Transactions on Industrial Electronics*, 57(12), 4001-4012, 2010.

Jae Sik Lim. Model predictive control of current and voltage for Li-Ion battery charger using 3-phase AC/DC converter. *In SICE Annual Conference*, 215-218, 2010.

W. Mo et al. Model predictive control for Z-source power converter. *In IEEE 8th International Conference on Power Electronics (ECCE)*, 3022-3028, 2011.

A. Vahidi et al. Current management in a hybrid fuel cell power system: A model predictive control approach. *IEEE Transactions on Control Systems Technology*, 14(6), 1047C1057, 2006.

Yanhui Xie et al. Implicit Model Predictive Control of a Full Bridge DCCDC Converter. *IEEE Transactions on Power Electronics*, 24(12), 2704-2713, 2009.

Y. Wang and Stephen Boyd. Fast model predictive control using online optimization. *Control Systems Technology*, 18(2), 267-278, 2010.

J. Rodriguez et al. Predictive current control of a voltage source inverter. *IEEE Transactions on Industrial Electronics*, 54(1), 495C503, 2007.

S. Alireza Davari et al. An Improved FCSCMPC Algorithm for an Induction Motor With an Imposed Optimized Weighting Factor. *IEEE Transactions on Power Electronic*, 27(3), 1540-1551.2012.

Petter THndela et al. An algorithm for multi-parametric quadratic programming and explicit MPC solutions. *Automatica*, 39(3), 489-497. 2003.

Ferrari-Trecate et al. Analysis of discrete-time piecewise affine and hybrid systems. *Automatica*, 38(12), 2139C2146, 2002.

Shi, Lisheng, and M. L. Crow. Comparison of ultracapacitor electric circuit models. *Power and Energy Society General Meeting-Conversion and Delivery of Electrical Energy in the 21st Century*, 1-6, 2008.

Mayne and Rakovi. Optimal Control of Constrained Piecewise Affine Discrete-Time Systems. Computational Optimization and Applications, Springer Berlin Heidelberg, 167-191, 2003.

Tobias Geyer et al. Hybrid Model Predictive Control of the Step-Down DCCDC Converter. *IEEE Transactions on Control Systems Technology*, 16(6), 1112-1124, 2008.

Anders Rantzer and Mikael Johansson. Piecewise linear quadratic optimal control. *Automatic Control*, 45(4), 629-637, 2000.

Borrelli. Constrained optimal control of linear and hybrid systems. Lecture notes in control and information sciences, Vol. 290, 2003.

Tondel et al. An algorithm for multi-parametric quadratic programming and explicit MPC solutions. *Automatica*, 39(3), 489-497, 2003.

Baotic et al. A new algorithm for constrained finite time optimal control of hybrid systems with a linear performance index. *In European control conference*, 3335-3340, 2003.

Geyer et al. Optimal complexity reduction of piecewise affine models based on hyperplane arrangements. *In American Control Conference*, 1190-1195, 2004.

Kvasnica et al. Multi-parametric toolbox (MPT). In Hybrid systems: computation and control, Springer Berlin Heidelberg, 448-462, 2004.